Regulation of DNMT1 stability through SET7-mediated lysine methylation in mammalian cells

Pierre-Olivier Estève[a,1], Hang Gyeong Chin[a,1], Jack Benner[a], George R. Feehery[a], Mala Samaranayake[a], Gregory A. Horwitz[b], Steven E. Jacobsen[b], and Sriharsa Pradhan[a,2]

[a]New England Biolabs Incorporated, 240 County Road, Ipswich, MA 01938; and [b]Howard Hughes Medical Institute and Department of Molecular, Cell, and Developmental Biology, University of California, Los Angeles, CA 90095-1606

Edited by Jasper Rine, University of California, Berkeley, CA, and approved February 10, 2009 (received for review October 15, 2008)

Inheritance of epigenetic information encoded by cytosine DNA methylation patterns is crucial for mammalian cell survival, in large part through the activity of the maintenance DNA methyltransferase (DNMT1). Here, we show that SET7, a known histone methyltransferase, is involved in the regulation of protein stability of DNMT1. SET7 colocalizes and directly interacts with DNMT1 and specifically monomethylates Lys-142 of DNMT1. Methylated DNMT1 peaks during the S and G_2 phases of the cell cycle and is prone to proteasome-mediated degradation. Overexpression of SET7 leads to decreased DNMT1 levels, and siRNA-mediated knockdown of SET7 stabilizes DNMT1. These results demonstrate that signaling through SET7 represents a means of DNMT1 enzyme turnover.

DNA methyltransferase | methylated lysine | proteasome | protein degradation

Mammalian DNA methylation is essential for development and is controlled by a variety of factors including 3 active DNA cytosine methyltransferases (DNMT1, DNMT3A, and DNMT3B) and a methyltransferase-like protein, DNMT3L (1–4). DNMT1 encodes the maintenance DNA methyltransferase (DNMT) responsible for methylating hemimethylated CpG sites shortly after DNA replication, and it is assisted by an accessory factor capable of recognizing hemimethylated DNA called UHRF1 (5, 6). Aberrant DNA methylation of CpG island-containing promoters leads to permanent silencing of genes in both physiological and pathological contexts and specifically in cancer cells (7). In cancer cells, disruption of DNMT1 resulted in hemimethylation of a fifth of the CpG sites in the genome and activation of the G_2/M checkpoint, leading to arrest in the G_2 phase of the cell cycle (8). Apart from DNA methylation-mediated gene silencing, DNMT1 also binds to several transcriptional inhibitors and represses gene expression in a DNA methylation-independent manner (9-11). Pharmacological inhibitors of DNMT1 [5-azacytidine (5-aza-CR) and its deoxy analog, 5-aza-2′-deoxycytidine (5-aza-CdR)] get incorporated into newly-synthesized DNA (12, 13). Once incorporated into DNA, these compounds form covalent complexes with DNMTs, thereby depleting active enzymes (14, 15) and activating gene expression (16). Recently, 5-aza-CdR-induced depletion of DNMT1 was shown to be mediated by proteasomal pathways in mammalian nuclei (17). However, little is known about other factors regulating DNMT1 levels in cells. Here, we show that DNMT1 stability is regulated by protein methylation coupled to proteasome-mediated protein degradation through the protein methyltransferase activity of SET7.

Results

DNMT1 Colocalizes and Associates with and Is Methylated by SET7. We used gel filtration and Western blot analysis to analyze DNMT1 from nuclear extracts. Using a highly-specific antibody we observed a major species of DNMT1 at 185 kDa and a higher molecular mass minor species (Fig. 1*A*). It seemed likely that this minor species of DNMT1 may be posttranslationally modified (18). To test whether DNMT1 might be modified by protein methylation, recombinant DNMT1 was incubated with *S*-adenosyl-L- [methyl-^{3}H] methionine (AdoMet) cofactor and several known catalytically-active histone methyltransferases (G9a, PRMT1, and SET7). In the SET7 reaction, a radioactive DNMT1 band along with degradation products was observed by fluorography (Fig. 1*B*). No band for radioactive DNMT1 was detected from samples incubated with either PRMT1 or G9a; however, H3 and H4 were detectable in all 3 lanes. These results suggest that SET7 methylates DNMT1.

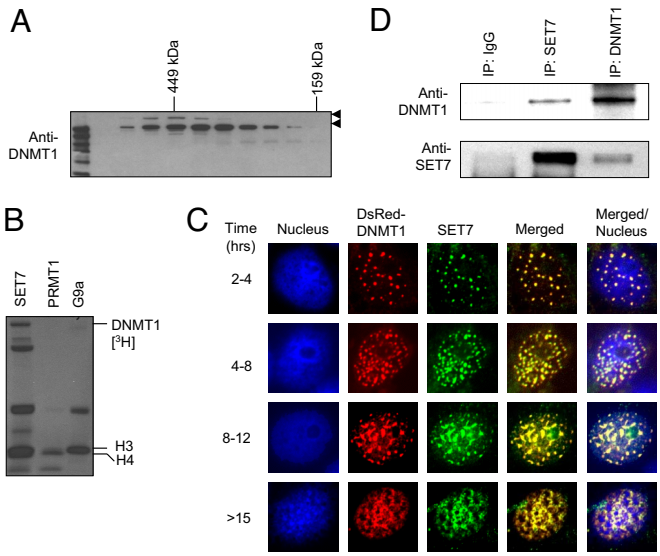

Fig. 1. DNMT1 association with SET7 and methylation by SET7. (*A*) Western blot analysis demonstrates 2 different species of DNMT1 eluted from gel filtration size exclusion chromatography of Jurkat cell nuclear extract as indicated. (*B*) Recombinant DNMT1 was incubated with ^{3}H[AdoMet] along with SET7, G9a, or PRMT1 followed by fluorography. (*C*) Transiently-expressed DsRed-DNMT1 (red) in COS-7 cells and endogenous SET7 (green) using an anti-SET7 antibody. Cells were released from G_1 arrest and followed for the time shown through S and G_2 phases. Nuclear staining was performed with Hoechst stain. (*D*) SET7 and DNMT1 coimmunoprecipitate as revealed by immunoprecipitations of SET7 or DNMT1 from nuclear extract of cells followed by Western blot analysis with the indicated antibodies.

Author contributions: G.A.H., S.E.J., and S.P. designed research; P.-O.E., H.G.C., J.B., G.R.F., and M.S. performed research; P.-O.E. and S.P. analyzed data; and S.E.J. and S.P. wrote the paper.

The authors declare no conflict of interest.

This article is a PNAS Direct Submission.

Freely available online through the PNAS open access option.

[1]P.-O.E. and H.G.C. contributed equally to this work.

[2]To whom correspondence should be addressed. E-mail: pradhan@neb.com.

This article contains supporting information online at www.pnas.org/cgi/content/full/0810362106/DCSupplemental.

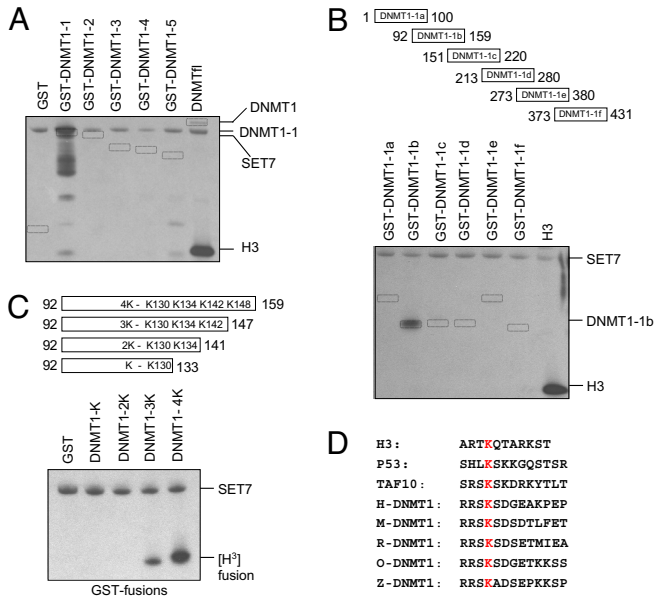

Fig. 2. Methylation analysis of the lysine residue on DNMT1. (*A*) Fluorography of GST fusion DNMT1 fragments (Fig. S1*A Upper*) in the presence of SET7 and ^{3}H[AdoMet]. DNMT1fl lane was spiked with *E. coli*-expressed recombinant H3 as an internal control. Note that SET7 is automethylated and the GST-DNMT1-1 fragment overlaps with SET7 but is methylated strongly. (*B*) Detailed mapping of the methylated lysine residue on GST-DNMT1-1 fragment. (*Upper*) GST fusion fragments schematically below the GST-DNMT1-1 and amino acid numbers. (*Lower*) The fluorography of the methylated fragments. H3 was included as a positive control. The gray shaded boxes in *A* and *B* are the trace of the fluorographed gel that was Coomassie-stained before processing. (*C*) Finer mapping and identification of the target lysine residue of SET7 methylation. Various DNMT1 GST-fusion constructs with 1–4 lysines (1K-4K) were incubated with ^{3}H[AdoMet] to determine the region of methylation by recombinant SET7. (*D*) Comparison of the consensus amino acids sequences surrounding the target lysine of DNMT1 that is methylated by SET7. The target lysine is shown in red. DNMT1s from human (H-DNMT1), mouse (M-DNMT1), rat (R-DNMT1), opossum (O-DNMT1), and zebrafish (Z-DNMT1), histone H3, p53, and TAF10 are shown.

If DNMT1 is a true in vivo substrate of SET7, these proteins would be predicted to colocalize and physically interact in nuclei. To study localization, DsRed-DNMT1-transfected COS-7 cells were fixed and immunostained for endogenous SET7. We found that DNMT1 and SET7 were significantly colocalized as evident by the punctate yellow merged pattern during the cell cycle (Fig. 1*C*), as was observed for DNMT1 and G9a (19). To investigate physical interaction, we immunoprecipitated both DNMT1 and SET7 and probed Western blots with anti-DNMT1 or anti-SET7. Results suggest a robust interaction between DNMT1 and SET7 (Fig. 1*D*). To determine whether this interaction is direct, a series of GST fusions covering the entire length of DNMT1 and SET7 were made and challenged with recombinant full-length proteins in GST pull-down assays. The amino terminus of SET7 interacted with both amino termini (amino acids 1–446) and carboxyl termini (amino acids 1081–1408) of DNMT1 (Fig. S1). Together, these results indicate that the DNMT1 and SET7 proteins interact.

SET7 Methylates K142 of DNMT1. We next sought to determine the precise residues in DNMT1 that are methylated by SET7. We incubated GST fusion fragments of DNMT1 with recombinant SET7 along with ^{3}H[AdoMet] and performed fluorography. We mapped the methylation site to an amino-terminal fragment of DNMT1 (GST–DNMT1-1; Fig. 2*A*), which was identical to 1 of the 2 fragments shown to directly interact with SET7 in the GST pull-down assays (Fig. S1). A detailed fluorography approach was undertaken to precisely map the lysine residue methylated by SET7. A fragment of DNMT1 representing amino acids 92–159 (GST–DNMT1-1b) with 4 lysines became methylated (Fig. 2*B*). A finer deletion mapping of GST–DNMT1-1b revealed Lys-142 (K142) representing an SKS motif as the target methylation site within DNMT1 (Fig. 2*C*). A homology search for similar motifs within DNMT1 identified another SKS motif at the carboxyl terminus (1093S1094K1095S). Interestingly, this motif did not display methylation by SET7 (Fig. 2*A*, DNMT1-4). We also compared sequences in the proximal vicinity of K142 of DNMT1 with amino acids residues surrounding SET7 methylation sites in histone H3 (20, 21), p53 (22), TAF10 (23), and DNMT1s from human, mouse, rat, zebrafish, and opossum. Amino acids sequence revealed that SET7 recognizes and methylates sequences T/L/S-K-Q/S/A (Fig. 2*D*).

SET7 Monomethylates K142 of DNMT1 at a Frequency Similar to H3K4. To determine the efficiency of SET7-mediated K142 methylation, peptides encompassing either DNMT1 Lys-142 (DNMT1K142) or encompassing Lys-4 of the tail histone H3 tail, a known substrate for SET7 (20), were used in steady-state kinetic assays. A constant amount of recombinant SET7 and ^{3}H[AdoMet] was used with increasing amounts of peptides. We found that the reaction progression curves for both substrates were very similar (Fig. 3*A*) with comparable catalytic efficiency (k_{cat}/K_{m}) and turnover (k_{cat}) values (H3K4: 2880^{-h}; DNMT1K142: 2520^{-h}; Fig. 3*B*), suggesting that DNMT1K142 is an efficient substrate for SET7. SET7 is known to add a single methyl group (monomethylation) to H3K4 (20, 21). Furthermore, we performed mass spectroscopic analysis of the time course of the reaction products and found that SET7 also predominantly monomethylates DNMT1K142 (Fig. 3*C*).

SET7 Modulates the DNMT1 Level in Mammalian Cells. To investigate DNMT1 methylation in vivo, we generated a rabbit polyclonal antibody specific for a methylated peptide encompassing K142. The antiserum was tested against in vitro-methylated DNMT1 by SET7 in the presence or absence of the cofactor AdoMet, thus making both DNMT1K142me and unmethylated protein. Results indicate that the antibody was capable of detecting DNMT1K142me robustly and did not cross-react with unmethylated DNMT1 (Fig. S2*a*). In the presence of K142me competitor peptide the signal was completely lost (Fig. S2*b*). The same blot probed by anti-DNMT1 antibody revealed comparable loading of both unmethylated and methylated DNMT1. Using this methylated DNMT1-specific antiserum (anti-DNMT1K142me), we performed cell cycle analysis of endogenous DNMT1K142me to determine the presence of methylated DNMT1 during the cell cycle. After being released from G_1 arrest, K142-methylated DNMT1 levels increased as cells progressed from early S to G_2 phase, mirroring the cell cycle-regulated marker cyclin A. Interestingly, levels of SET7 remained approximately constant throughout the cell cycle (Fig. 4*A*), suggesting that cell cycle-regulated methylation of DNMT1 may be regulated by cell cycle-specific communication between SET7 and DNMT1.

To investigate the functional consequences of SET7-mediated methylation of DNMT1, we performed knockdown of SET7 in HeLa cells by using RNAi duplex (Si-SET7). A strong knockdown of SET7 protein was observed, which correlated with a similar reduction in mRNA levels (Fig. 4 *B* and *C*). Surprisingly, we found that the DNMT1 protein levels, but not the mRNA levels, increased in the SET7 knockdown cells (Fig. 4*B*), suggesting that DNMT1 K142 methylation may regulate the stability of DNMT1. This hypothesis would predict that overexpression of SET7 would cause DNMT1 degradation. To test this idea, we cotransfected either wild-type DNMT1 (DsRed-DNMT1) or a DNMT1 mutant (DsRed-DNMT1K142A) that cannot be meth-

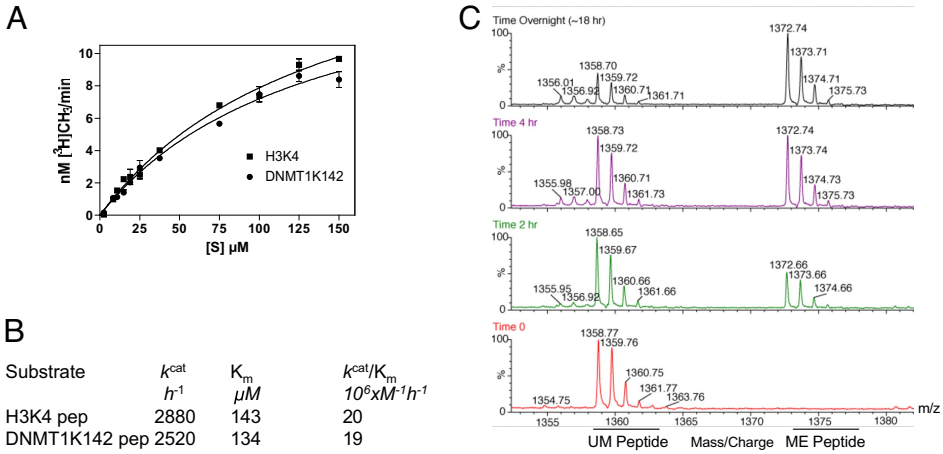

B

Substrate	k^{cat} h^{-1}	K_m μM	k^{cat}/K_m $10^6 x M^{-1} h^{-1}$
H3K4 pep	2880	143	20
DNMT1K142 pep	2520	134	19

Fig. 3. Comparison of methylation rate between H3 and DNMT1 and identification of the methylation specificity of SET7 using DNMT1 peptide. (*A*) Steady-state kinetic analysis of H3K4 and DNMT1K142 peptide substrate [S] with SET7. (*B*) Comparison of the kinetic constants between H3K4 peptide and DNMT1 peptide representing K142 region. (*C*) Time course of DNMT1K142 peptide methylation assayed by mass spectrometry. The starting peptide material unmethylated (UM) peptide and reaction product methylated (ME) peptide is shown at the bottom.

ylated by SET7 into COS-7 cells together with either a GFP-SET7 functional protein or a control GFP alone (Fig. 4*D*). The DsRed-DNMT1 is larger than endogenous DNMT1 and thus can be distinguished by Western blot analysis. We found that wild-type DsRed-DNMT1 was methylated by GFP-SET7 (Fig. 4*D*, anti-DNMT1K142me, lane 4) and degraded, as compared with the K142 mutant (Fig. 4*D*, anti-DNMT1, lanes 2 vs. 4). These results suggest that K142 methylation of DNMT1 by SET7 plays a role in DNMT1 stability and degradation.

Because overexpression of SET7 degrades cellular DNMT1, a reduction of genomic DNA methylation is strongly predicted. To test this hypothesis, genomic DNA from HeLa cells transfected with control or SET7 were examined for methylation changes. We first used a nucleotide analysis via HPLC to determine global demethylation changes. We observed that genomic DNA extracted from cells overexpressing SET7 were ≈10% hypomethylated, suggesting that global levels of methylation were decreased in SET7-overexpressing cells (Fig. S3*A*). Furthermore, we used a methylation-specific PCR (MSP) assay (24) at 2 individual loci (*RARβ2* and *rDNA*) that have been shown to be possible DNMT1 target sequences (25, 26), and we observed partial demethylation of all of the loci in SET7-overexpressing cells (Fig. S3*B*).

We next sought to determine the mechanism by which K142 methylation of DNMT1 stimulates DNMT1 degradation. COS-7-transfected cells were treated with the protein synthesis inhibitor cycloheximide, so that we could follow DNMT1 degradation patterns by Western blot analysis without the complication of additional DNMT1 protein synthesis (Fig. 4*E*). Results demonstrate that wild-type DNMT1-DsRed decreased, whereas the K142A mutant DNMT1 levels were stabilized (Fig. 4*E*, lanes 3 vs. 6). Interestingly, both wild-type and DNMT1K142A mutant displayed a similar cell cycle-dependent replication fork association (Fig. S4), suggesting that K142 methylation affects DNMT1 stability but not its replication fork loading or nuclear localization (27, 28). Furthermore, the half-life of methylated DNMT1 and unmethylated DNMT1 stability were determined by quantitative analysis. Cycloheximide-treated Jurkat cell extracts were analyzed by Western blot and probed with anti-DNMT1 (K142me) or anti-DNMT1 antibodies. Indeed, the methylated DNMT1 degradation was much faster than the unmethylated enzyme. Methylated DNMT1 displayed a shorter half-life (2–6 h) as compared with unmethylated DNMT1 (12–24 h; Fig. S5*A*). Similarly, in a pulse–chase experiment using transfected wild-type and mutant K142A DNMT1 constructs, we observed that the wild-type DNMT1 is prone to degradation (half-life ≈9–12 h) as compared with the mutant enzyme K142A, which displayed a half-life >24 h (Fig. S5*B*). Therefore, mutation on DNMT1 K142A stabilizes the protein and acts as a negative modulator for proteasome-mediated degradation.

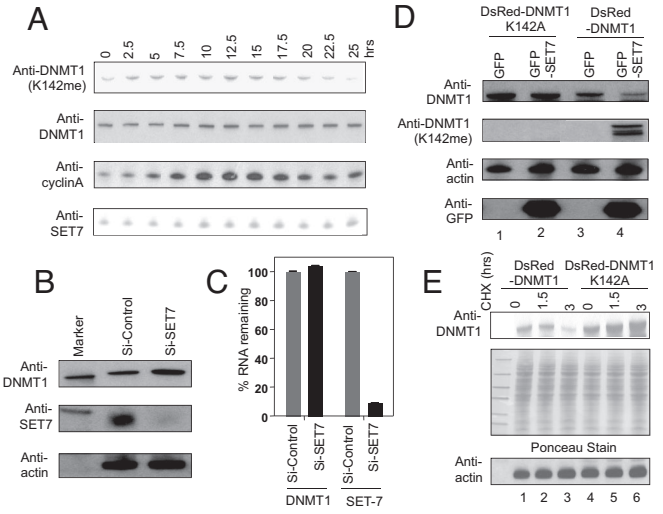

Fig. 4. SET7-mediated DNMT1 methylation in mammalian cells (*A*) Cell cycle expression analysis of SET7, cyclin A, total DNMT1, and DNMT1K142me in synchronized cells released from G_1 arrest. (*B*) HeLa cells with SET7 knockdown (Si-SET7) or control knockdown (Si-Control) followed by Western blot analysis with the indicated antibodies. (*C*) The mRNA level of DNMT1 and SET7 in control and Si-SET7 knockdown cells. (*D*) Overexpression of SET7 (GFP-SET7), DNMT1 (DsRed-DNMT1), or a DNMT1 mutant (DsRed-DNMT1K142A) in cells followed by Western blot analysis with the indicated antibodies. Anti-actin was used as a loading control, while anti-GFP demonstrates equal expression of GFP-SET7. (*E*) DNMT1 (DsRed-DNMT1)- or DNMT1 mutant (DsRed-DNMT1K142A)-transfected cells were treated for the indicated times with 10 μg/mL cycloheximide (CHX) followed by Western blot analysis with anti-DNMT1. Equal loading is indicated by ponceau stain and Western blot with anti-actin.

Proteasome-Mediated Degradation of DNMT1 Is Facilitated by SET7. Because DNMT1 degradation relies on K142 methylation in DNMT1, we next examined whether ubiquitin-mediated degradation plays a role in enzyme stability. Previous study with the

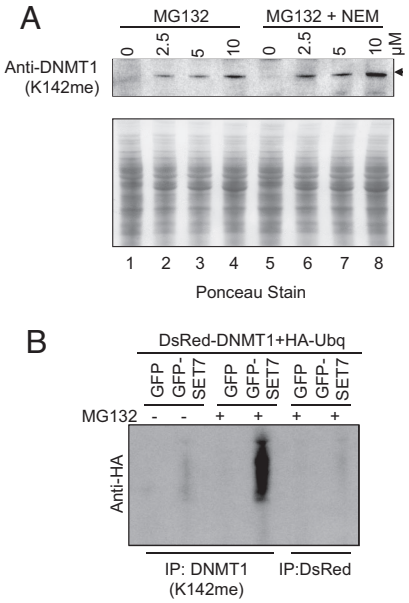

Fig. 5. Lysine methylation of DNMT1 facilitates proteasome mediated DNMT1 degradation. (*A*) Cells were treated with MG132 and lysed with or without the proteinase inhibitor NEM followed by Western blot analysis with the indicated antibodies. Ponceau stain demonstrates equal loading. (*B*) Cells overexpressing DNMT1, HA-ubiquitin, and control GFP or GFP-SET7 in the presence or absence of the proteasome inhibitor MG132 followed by immunoprecipitation (IP) of the nuclear extract and Western blot analysis with anti-HA antibody.

proteasome inhibitor MG132 suggested that the degradation of DNMT1 was reduced, indicating that DNMT1 degradation is mediated by the ubiquitin–proteasome pathway (17). To confirm these findings with endogenous DNMT1, Western blot analysis was performed with anti-DNMT1K142me antibody on extracts from HeLa cells treated with MG132 in the presence or absence of the proteinase inhibitor *N*-ethylmaleimide (NEM) (Fig. 5*A*). In the absence of MG132 (Fig. 5*A*, lanes 1 and 5), complete degradation of methylated DNMT1 (DNMT1K142me) was observed, confirming that methylated DNMT1 is the target for protein degradation. Addition of MG132 alone or NEM together with MG132 (which allows further accumulation of DNMT1) resulted in dose-dependent accumulation of DNMT1K142me (Fig. 5*A*). Overall, these results strongly suggest that K142-methylated DNMT1 is degraded by the ubiquitin–proteasome pathway.

Because the majority of cellular proteins destined for degradation are polyubiquitylated (29), we examined whether proteasome-mediated degradation of DNMT1K142me is associated with polyubiquitylation. Methylated DNMT1 was immunoprecipitated by using anti-DNMT1K142me from COS-7 cells cotransfected with HA-tagged ubiquitin and DsRed-DNMT1 along with GFP or GFP-SET7. Anti-HA was then used to detect ubiquitinylated proteins. A strong HA signal was seen only in cells transfected with GFP-SET7 in the presence of MG132, confirming that methylated DNMT1 is the substrate for ubiquitylation (Fig. 5*B*). Furthermore, the higher molecular mass smear of signal indicated the presence of polyubiquitin (Fig. 5*B*), which suggests that SET7-mediated DNMT1 methylation triggers DNMT1 polyubiquitylation. Similar polyubiquitylation of DNMT1 was observed in mammalian cells treated with lactacystin, another proteasome inhibitor (17).

Discussion

Our results suggest that signaling through SET7-mediated methylation of DNMT1 regulates proteasome-mediated degradation of DNMT1. The DNMT1K142me degradation mechanism is in contrast with SET7-mediated TAF-10 and p53 methylation. In both cases, lysine methylation is required for their structural/functional stabilization. Monomethyl TAF10 has an increased affinity for RNA polymerase II and is involved in preinitiation complex formation on some TAF10-dependent genes. Similarly, monomethylation of the carboxyl-terminus lysine in p53 protein increases its structural stability perhaps via recruiting monomethyl p53 binding protein that can interfere with MDM2-mediated ubiquitination. Furthermore, Set7-mediated methylation regulates the expression of p53 target genes in a manner dependent on p53 methylation.

Although it is clear that DNMT1 is an in vivo methylation target of SET7, the in vivo role of DNMT1 methylation is thus far unclear. A mouse knockout of Set7 was recently reported to show normal development through adulthood. However, Set7 null cells did not follow normal cell cycle arrest after DNA damage, implying deregulation of cell cycle check points (30). Because our data suggest that DNMT1 would lack methylation and be more stable in the SET7 deletion strains, and yet no dramatic phenotypic consequences are seen, these results suggest that DNMT1 methylation may play a subtle role in DNA methylation control, or one that is only observed under certain conditions. One speculative hypothesis for the function of DNMT1 methylation could be its clearance from methylated promoters when a previously methylated and silent gene is first becoming expressed. In this case, SET7-mediated DNMT1 degradation may not be strictly required for gene activation, but might alter the kinetics of the process. An analogous situation would be H3K4 methylation in the yeast *Saccharomyces cerevisiae*. Even though SET1 (the H3K4 methyltransferase) deletion strains grow normally, the kinetics of gene activation is slower than in the wild type (31). Recently, loss of genomic methylation in targeted deletion of LSD1 (*Aof2*) in mouse ES cells was shown (32). In that study, the loss of DNA methylation correlated with degradation of Dnmt1 caused by K1096 methylation by Set7. However, in human DNMT1 K142 is the major target site for SET7 resulting in its degradation. Thus, both mouse and human enzyme may follow the same mechanistic pathway for DNMT1 degradation via different lys methylation. Although future research should help clarify the SET7 target amino acid residues and the role of DNMT1 methylation, the data reported here suggest that SET7-mediated degradation of DNMT1 and hypomethylation of the genome may be a fine-tuning mechanism resulting in epigenetic modulation of gene expression.

Materials and Methods

Cell Culture, Cell Cycle, Protein Stability, GST Pull-Down, Immunoprecipitation, and Immunocytochemistry. All cell lines (HeLa and COS-7) were obtained from the ATCC and were grown per recommendations. Cells were synchronized in G_1/S by using 2 mM Thymidine block followed by 0.4 mM Mimosine treatment. For DsRed-DNMT1 protein stability studies, COS-7 cells were transfected with a mixture of transpass D2 transfection reagent (NEB) and DsRed-DNMT1 or DsRed-DNMT1-K142A plasmid at a ratio of 1:3 μg/μL for 48 h. Cells were then treated with 10 μg/mL cycloheximide (Sigma), lysed, and assayed by Western blot analysis using a DNMT1 antibody (NEB).

Immunoprecipitation of nuclear cell extract were performed according to Estève et al. (19), by using 2 μg each of anti-DNMT1 (NEB), anti-SET7 (CST), anti-DsRed antibody (Biovision) or 5 μL of antiserum raised against DNMT1K142me (NEB). Two micrograms of purified rabbit IgG (Jackson Laboratory) was used as negative control. Nuclear extracts were made as described (33).

GST pull-downs were performed as described (34). DNMT1 and SET7 were obtained from NEB. SET7 was cloned into pVIC1 (NEB) and purified as described by Pradhan et al. (35).

For immunofluorescence studies, COS-7 cells were cultured on coverslips and transfected with a mixture of DsRed-DNMT1 or DsRed-DNMT1-K142A plasmid and Transpass D2 transfection reagent (NEB) at a ratio of 1:3 μg/μL for 24 h. The cells were then synchronized in G_1/S and after fixation were visualized with a Zeiss 200 M microscope with 63× oil objective lens at 568 nm for

DsRed-DNMT1 and 460 nm for nuclear staining using Hoechst 33342. Endogenous SET7 or proliferating cell nuclear antigen (PCNA) were detected by anti-SET7 or anti-PCNA (CST) and secondary antibodies anti-rabbit IgG or anti-mouse IgG conjugated with AlexaFluor 488 nm (Molecular Probes), respectively.

Gel Filtration Chromatography. Gel filtration chromatography was performed with Jurkat cell nuclear extract as described by Estève et al. (19).

Methyltransferase Assay, Mass Spectroscopy, and Fluorography. Methyltransferase assays were carried out at 37 °C for 10 min in duplicate with a total volume of 25 μL of reaction mix. A typical reaction contained AdoMet (specific activity 15 Ci/mmol; Amersham), substrate peptide, and SET7 enzyme (NEB) in assay buffer (NEB). Peptide substrates were used for methyltransferase assay. Peptides representing histone H3 amino terminus tail (H3K4): CARTKQTARKSTGG and DNMT1 (DNMT1K142): RTPRRSKSDGEA were dissolved in water. The reactions were stopped by transferring the reaction tubes to an ethanol-dry ice bath and were processed by spotting the reaction mix on PE81 paper circles (Whatman). These circles were washed sequentially with 3 $\times$ 1 mL of cold 0.2 M ammonium bicarbonate, 3 $\times$ 1 mL of Milli Q water, and 3 $\times$ 1 mL of ethanol using a manifold (Millipore) connected to a vacuum pump. The filters were dried, 3 mL of Safe Scint (American Bioanalytical) was added to each, and tritium incorporation was measured.

For mass spectroscopy analysis the methylated peptides were prepared by using Fmoc chemistry as per Estève et al. (36). The spectra were obtained on an Agilent ion trap 6330 LC/MS system.

Fluorography of the radioactive samples were performed as described (37), except the samples were GST-fused DNMT1 fragments/recombinant DNMT1 (NEB). Each methyltransferase assay for fluorography was performed with 500 ng of the fusion protein overnight at room temperature.

Proteasome Inhibitor Treatment, Western Blot Analysis, SiRNA Knockdown, and Quantitative PCR Analysis. HeLa or COS-7 cells cotransfected with GFP or GFP-SET7 and HA-Ubiquitin plasmids were treated with different concentrations of proteasome inhibitor MG132 (Calbiochem) for 24 h. The HeLa cells were then lysed by using RIPA buffer (0.15 M NaCl/0.05 M Tris-HCl, pH 8.0/0.02% NaN3/1% NP40) containing 1X protease inhibitor cocktail (Sigma)/5 mM PMSF and 100 μM NEM (Sigma) and assayed for Western blot analysis. Transfected COS-7 cells were treated with 10 μM MG132 for 24 h and lysed by using the protocol described by Andrews and Faller (33) in the presence of 100 μM NEM.

Western blot analysis was performed according to Estève et al. (19). Antibodies and antiserum against DNMT1 were obtained from NEB. Anti-SET7, anti-cyclin A, and anti-HA tags were obtained from CST. Anti-actin and anti-GFP monoclonal antibodies were obtained from Sigma and Roche Applied Science, respectively.

For *SET7* gene knockdown, HeLa cells were transfected 3 times by using Transpass HeLa reagent (NEB) with 20 nM validated Stealth RNAi duplex RNA (Invitrogen). For control transfection, a Stealth RNAi negative control was used (Invitrogen). Cells were then harvested, and total RNA was purified by the RNeasy kit (Qiagen). The ProtoScript First-Strand cDNA Synthesis Kit (NEB) was used to produce cDNA. RNA quantization was performed by real-time PCR, using a MyiQ Cycler (Bio-Rad) and iQ SYBR Green Supermix (Bio-Rad) using primers GGCTGAGATGAGGCAAAAAG (forward) and ACCAACTCGGTACAGGATGC (reverse) for DNMT1 and CGTGGTGTGCCTGAGCCCTATAACCACG (forward) and TGAAGGAGTGATTTGCCTTGTGT (reverse) for SET7. RNA values were normalized by using primers for human ALDOA: CGGGAAGAAGGAGAACCTG (forward) and GACCGCTCGGAGTGTACTTT (reverse). The percentage of mRNA remaining was compared with cells treated with Stealth RNAi negative control (Invitrogen). Error bars on the graphs represent standard deviation of 3 independent experiments.

Transient Transfection and MSP. HeLa cells were transfected 3 times for 48 h with a mixture of GFP or GFP-SET7 plasmid and Transpass HeLa transfection reagent (NEB) at a ratio of 1:3 μg/μL. Genomic DNA was then extracted with a DNeasy blood and tissue kit (Qiagen). Four micrograms of the genomic DNA was bisulfite-treated with an EpiTect Bisulfite kit (Qiagen). MSP were performed according to Estève et al. (19). Primers for MSP are available on request. U and M represents unmethylated and methylated primer sets, respectively, for MSP assay.

DNMT1 Stability Assay. DNMT1 stability was determined by pulse–chase assay. COS-7 cells were transfected with DsRed-DNMT1- or DsRed-DNMT1(K142A)-encoding plasmids by using Transpass D2 reagent (NEB). After 24-h transfection, cells were labeled with [^{35}S]methionine (20 μCi/mL; NEN) for 8 h in methionine-free DMEM, washed with 1$\times$ PBS, and chased with DMEM containing 0.2 mM methionine. After cell nuclear extraction, 200 μg of nuclear extract was used for DNMT1 immunoprecipitation using 2 μg of DsRed antibody (Biovision) overnight at 4 °C. The immuno complex was captured with 35 μL of protein-G agarose (KPL) blocked with BSA for 2 h and washed once with 1$\times$ PBS and subsequently once again with 1$\times$ PBS containing 500 mM NaCl. The beads were then resuspended with 30 μL of SDS sample buffer supplemented with DTT. After boiling the samples, 10 μl was loaded on a 10% SDS-Tricine gel. After fluorography, gels were dried and exposed to Kodak Biomax MS films at $-$70 °C for 5 days.

ACKNOWLEDGMENTS. We thank Rich Roberts, Bill Jack, Don Comb, and New England Biolabs for research support and Magnolia Bostick and Jong Kyong Kim for technical assistance. Work in S.E.J.'s laboratory is supported by National Institutes of Health Grant GM60398. S.E.J. is an Investigator of the Howard Hughes Medical Institute. G.A.H. is supported by National Cancer Institute Award F32CA137995.

1. Li E, Bestor TH, Jaenisch R (1992) Targeted mutation of the DNA methyltransferase gene results in embryonic lethality. *Cell* 69:915–926.
2. Okano M, Bell DW, Haber DA, Li E (1999) DNA methyltransferases Dnmt3a and Dnmt3b are essential for de novo methylation and mammalian development. *Cell* 99:247–257.
3. Bestor T, Laudano A, Mattaliano R, Ingram V (1988) Cloning and sequencing of a cDNA encoding DNA methyltransferase of mouse cells. The carboxyl-terminal domain of the mammalian enzymes is related to bacterial restriction methyltransferases. *J Mol Biol* 203:971–983.
4. Okano M, Xie S, Li E (1998) Cloning and characterization of a family of novel mammalian DNA (cytosine-5) methyltransferases. *Nat Genet* 19:219–220.
5. Bostick M, et al. (2007) *UHRF1* plays a role in maintaining DNA methylation in mammalian cells. *Science* 317:1760–1764.
6. Sharif J, et al. (2007) The SRA protein Np95 mediates epigenetic inheritance by recruiting Dnmt1 to methylated DNA. *Nature* 450:908–912.
7. Baylin SB, Ohm JE (2006) Epigenetic gene silencing in cancer: A mechanism for early oncogenic pathway addiction? *Nat Rev Cancer* 6:107–116.
8. Chen T, et al. (2007) Complete inactivation of DNMT1 leads to mitotic catastrophe in human cancer cells. *Nat Genet* 39:391–396.
9. Fuks F, Burgers WA, Brehm A, Hughes-Davies L, Kouzarides T (2000) DNA methyltransferase Dnmt1 associates with histone deacetylase activity. *Nat Genet* 24:88–91.
10. Fuks F, et al. (2003) The methyl-CpG-binding protein MeCP2 links DNA methylation to histone methylation. *J Biol Chem* 278:4035–4040.
11. Robertson KD, et al. (2000) DNMT1 forms a complex with Rb, E2F1, and HDAC1 and represses transcription from E2F-responsive promoters. *Nat Genet* 25:338–342.
12. Bouchard J, Momparler RL (1983) Incorporation of 5-Aza-2′-deoxycytidine-5′-triphosphate into DNA. Interactions with mammalian DNA polymerase α and DNA methylase. *Mol Pharmacol* 24:109–114.
13. Jüttermann R, Li E, Jaenisch R (1994) Toxicity of 5-aza-2′-deoxycytidine to mammalian cells is mediated primarily by covalent trapping of DNA methyltransferase rather than DNA demethylation. *Proc Natl Acad Sci USA* 91:11797–11801.
14. Santi DV, Garrett CE, Barr PJ (1983) On the mechanism of inhibition of DNA-cytosine methyltransferases by cytosine analogs. *Cell* 33:9–10.
15. Santi DV, Norment A, Garrett CE (1984) Covalent bond formation between a DNA-cytosine methyltransferase and DNA containing 5-azacytosine. *Proc Natl Acad Sci USA* 81:6993–6997.
16. Chuang JC, et al. (2005) Comparison of biological effects of non-nucleoside DNA methylation inhibitors versus 5-aza-2′-deoxycytidine. *Mol Cancer Ther* 4:1515–1520.
17. Ghoshal K, et al. (2005) 5-Aza-deoxycytidine induces selective degradation of DNA methyltransferase 1 by a proteasomal pathway that requires the KEN box, bromo-adjacent homology domain, and nuclear localization signal. *Mol Cell Biol* 25:4727–4741.
18. Beausoleil SA, et al. (2004) Large-scale characterization of HeLa cell nuclear phosphoproteins. *Proc Natl Acad Sci USA* 101:12130–12135.
19. Estève P-O, et al. (2006) Direct interaction between DNMT1 and G9a coordinates DNA and histone methylation during replication. *Genes Dev* 20:3089–3103.
20. Wang H, et al. (2001) Purification and functional characterization of a histone H3-lysine 4-specific methyltransferase. *Mol Cell* 8:1207–1217.
21. Nishioka K, et al. (2002) Set9, a novel histone H3 methyltransferase that facilitates transcription by precluding histone tail modifications required for heterochromatin formation. *Genes Dev* 16:479–489.
22. Chuikov S, et al. (2004) Regulation of p53 activity through lysine methylation. *Nature* 432:353–360.
23. Kouskouti A, Scheer E, Staub A, Tora L, Talianidis I (2004) Gene-specific modulation of TAF10 function by SET9-mediated methylation. *Mol Cell* 14:175–182.

24. Herman JG, Graff JR, Myöhänen S, Nelkin BD, Baylin SB (1996) Methylation-specific PCR: A novel PCR assay for methylation status of CpG islands. *Proc Natl Acad Sci USA* 93:9821–9826.
25. Di Croce L, et al. (2002) Methyltransferase recruitment and DNA hypermethylation of target promoters by an oncogenic transcription factor. *Science* 295:1079–1082.
26. Santoro R, Li J, Grummt I (2002) The nucleolar remodeling complex NoRC mediates heterochromatin formation and silencing of ribosomal gene transcription. *Nat Genet* 32:393–396.
27. Chuang LS, et al. (1997) Human DNA-(cytosine-5) methyltransferase–PCNA complex as a target for p21WAF1. *Science* 277:1996–2000.
28. Leonhardt H, Page AW, Weier HU, Bestor TH (1992) A targeting sequence directs DNA methyltransferase to sites of DNA replication in mammalian nuclei. *Cell* 71:865–873.
29. Hershko A, Ciechanover A (1998) The ubiquitin system. *Annu Rev Biochem* 67:425–479.
30. Kurash JK, et al. (2008) Methylation of p53 by Set7/9 mediates p53 acetylation and activity in vivo. *Mol Cell* 29:392–400.
31. Fleming AB, Kao CF, Hillyer C, Pikaart M, Osley MA (2008) H2B ubiquitylation plays a role in nucleosome dynamics during transcription elongation. *Mol Cell* 31:57–66.
32. Wang J, et al. (2009) The lysine demethylase LSD1 (KDM1) is required for maintenance of global DNA methylation. *Nat Genet* 41:125–129.
33. Andrews NC, Faller DV (1991) A rapid micropreparation technique for extraction of DNA-binding proteins from limiting numbers of mammalian cells. *Nucleic Acids Res* 19:2499.
34. Kim G-D, Ni JW, Stark N, Roberts RJ, Pradhan S (2002) Cooperation and communication between the human maintenance and de novo DNA (cytosine-5) methyltransferases. *EMBO J* 21:4183–4195.
35. Pradhan S, Bacolla A, Wells RD, Roberts RJ (1999) Recombinant human DNA (cytosine-5) methyltransferase. I. Expression, purification, and comparison of de novo and maintenance methylation. *J Biol Chem* 274:33002–33010.
36. Estève P-O, et al. (2005) Functional analysis of the N and C terminus of mammalian G9a histone H3 methyltransferase. *Nucleic Acids Res* 33:3211–3223.
37. Chin HG, et al. (2005) Sequence specificity and role of proximal amino acids of the histone H3 tail on catalysis of murine G9A lysine 9 histone H3 methyltransferase. *Biochemistry* 44:12998–13006.